

CONTINUATION LOAD FLOW WITH A NEURO FUZZY MODEL OF AN INDUCTION MOTOR FOR VOLTAGE STABILITY ANALYSIS

Muriithi C. M ^{#1}, Ngoo L. M ^{*2}, Nyakoe G. N ^{#3}, Njoroge S. N ^{*4}

Department of Electrical & Electronics
Jomo Kenyatta University of Agriculture & Technology
Nairobi, Kenya

¹cmmuriithi@eng.jkuat.ac.ke, ²mwalungoo@yahoo.com, ³nyakoe@eng.jkuat.ac.ke, ⁴lechnjugunatss@hotmail.com

Abstract: This paper uses the concept of the continuation power flow analysis used in voltage stability analysis for control the power in large systems. It uses the $P-V$ curves to find the knee point of a certain bus. A neuro-fuzzy model of an induction motor load is used to represent an industrial load. In the subsequent predictor-corrector stages, the induction motors are increased to depict increment in loading. Different motor ratings are used in the investigations. The process starts at some base values of the system and leading to the critical point. Further the reduced Jacobian is used to determine the optimum location for capacitor to affect maximum voltage improvement in total over a range of operating points. In case study, illustrative examples with the IEEE 30 bus system are shown.

Key Words: Continuation Load Flow, Induction Motors, Voltage Stability

1. INTRODUCTION

As power systems become more complex and heavily loaded, voltage stability becomes an increasing serious problem. Voltage problems have been a subject of great concern during planning and operation of power systems due to the significant number of serious failures believed to have been caused by this phenomenon. It is therefore necessary to develop Voltage Stability Analysis (VSA) tools in today's Energy Management Systems (EMS). [1]

The continuation power flow [2], as known, is a useful tool to plot the entire P-V curve. The continuation power flow uses a predictor-corrector scheme [2] to solve the set of load flow equations which are reformulated to accommodate a load parameter λ which denotes the increase in load from the base point.

In [3], the conventional load flow algorithm has been modified to incorporate a neuro fuzzy model of an induction motor load (IM), which updates the reactive power and slip

during each iteration. In this modification the reactive power of the IM load which is a function of its voltage is accurately estimated, which is not the case in the conventional load flow solution [4]. It is revealed in [5] that modeling industrial loads as motors allows better analysis of the system behavior and improves the ability to reveal voltage stability problems.

Reactive power compensation with components like capacitors is a trend popular in power systems today so as to ensure the continuous system reliability, given the regular overloading and the resulting lack of reactive power supply and voltage collapse. The use of these components however, is not a subject of free choice since these components are expensive. In [6] the reduced Jacobian is derived for V-Q sensitivity analysis. The technique is extended in [1] by implementing a simple computation on the elements of the reduced Jacobian to find the suitable bus for capacitor placement.

This paper demonstrates how the neuro fuzzy model of the induction motor can be incorporated in the continuation load flow where the singularity in the Jacobian can be avoided by slightly reformulating the power flow equations and applying a locally parameterized continuation technique [2]. Further, different induction motor ratings are used to plot the PV and QV curves. The results indicate that though the PV curves have almost similar maximum loading, but the QV curves are different for motor ratings. Specifically, large induction motors consume less reactive power at base values, but as loading continues, the consumption increases drastically leading to stressed buses in terms of voltage stability. During the continuation power flow, the reduced Jacobian is formulated and the bus numbers deemed best for capacitor placement at the operating points are determined.

The paper is organized as follows. In section 2, we discuss the Mathematical Formulation, section 3, we conducted a case study using the IEEE 30 bus system; section 4, we outline the conclusions.

2. MATHEMATICAL FORMULATION

A. REFORMULATION OF THE POWER FLOW EQUATIONS

In order to apply a locally parameterized continuation technique to the power flow problem, a load parameter must be inserted into the equations [2]. While there are many ways this could be done, only a simple example using a constant power load model will be considered here.

First let λ represent the load parameter such that

$$0 \leq \lambda \leq \lambda_{critical} \quad (1)$$

Where $\lambda = 0$ corresponds to the base load and $\lambda = \lambda_{critical}$ corresponds to the critical load. We desire to incorporate λ into

$$0 = P_{Gi} - P_{Li} - P_{Ti}, P_{Ti} = \sum_{j=1}^n V_i V_j y_{ij} \cos(\delta_i - \delta_j - v_{ij}) \quad (2)$$

$$0 = Q_{Gi} - Q_{Li} - Q_{Ti}, Q_{Ti} = \sum_{j=1}^n V_i V_j y_{ij} \sin(\delta_i - \delta_j - v_{ij}) \quad (3)$$

for each bus i of an n bus system, where the subscripts L , G , and T denote bus load, generation and injection respectively. The voltages at buses i and j are $V_i \angle \delta_i$ and $V_j \angle \delta_j$ respectively and $y_{ij} \angle v_{ij}$ is the $(i, j)^{th}$ element of Y_{BUS} .

To simulate a load change, the P_{Li} and Q_{Li} terms must be modified. This can be done by breaking each term into two components. One component will correspond to the original load at bus i and the other component will represent a load change brought about by a change in the load parameter λ .

Thus,

$$P_{Li} = P_{Li0} + \lambda(K_{Li} S_{\Delta base} \cos \psi_i) \quad (4)$$

$$Q_{Li} = Q_{Li0} + \lambda(K_{Li} S_{\Delta base} \sin \psi_i) \quad (5)$$

Where the following definitions are made;

P_{Li0} , Q_{Li0} – original load at bus i , active and reactive respectively.

K_{Li} – multiplier to designate the rate of load change at bus i as λ changes.

ψ_i – power factor angle of load change at bus i .

$S_{\Delta base}$ – a given quantity of apparent power which is chosen to provide appropriate scaling of λ .

For the induction motor load, P_{Li} is the scheduled load out of which the number of induction motors to be aggregated is estimated. This is done by dividing the scheduled power with the induction motor rating being investigated. The aggregation is done using equations detailed in [7].

In addition, the active power generation term can be modified to

$$P_{Gi} = P_{Gi0} (1 + \lambda K_{Gi}) \quad (7)$$

where P_{Gi} is the active generation at bus i in the base case and K_{Gi} is a constant used to specify the rate of change in generation as λ varies.

If these new expressions are substituted into the power flow equations, the result is

$$0 = P_{Gi0} (1 + \lambda K_{Gi}) - P_{Li0} - \lambda (K_{Li} S_{\Delta base} \cos \psi_i) - P_{Ti} \quad (8)$$

$$0 = Q_{Gi0} - Q_{Li0} - \lambda (K_{Li} S_{\Delta base} \sin \psi_i) - Q_{Ti} \quad (9)$$

Notice that values of K_{Li} , K_{Gi} , and ψ_i can be uniquely specified for every bus in the system. This allows for a very specific variation of load and generation as λ changes.

B. NEURO-FUZZY MODEL OF AN INDUCTION MOTOR LOAD

To get neuro-fuzzy model of an induction motor load, the power balance equation (6) which is non-linear is solved to get the operating slip at each voltage.

$$P_{elect} - P_{mech} = 0 \quad (6)$$

The operating slip is used to calculate the active and reactive power consumed at the load bus at each voltage. The Artificial Neuro Fuzzy Inference System is then used to map both the active and reactive power at operating slips to the respective voltages. The algorithm for creating the neuro-fuzzy model of the induction motor as detailed in [6] is summarized in Fig. A1 in the appendix.

C. THE APPLICATION OF A CONTINUATION ALGORITHM

The method of continuation power flow [2,6] is dealt with in brief here. The power flow equations for a particular bus i were reformulated to contain a load parameter λ . The next step is to apply a continuation algorithm to the system of reformulated power flow equations. If \underline{F} is used to denote the whole set of equations, the problem can be expressed as

$$F(\underline{\varrho}, \underline{V}, \lambda) = 0, \quad 0 \leq \lambda \leq \lambda_{critical} \quad (10)$$

where $\underline{\varrho}$ represents the vector of bus voltage angles and \underline{V} represents the vector of bus voltage magnitudes. As mentioned,

the base case solution $(\underline{\delta}_o, \underline{V}_o, \lambda_o)$ is known via a conventional power flow and the solution path is being sought over a range of λ . In general, the dimensions of F will $2n1 + n2$, where $n1$ and $n2$ are the number of P - Q and P - V buses respectively.

To solve the problem, the continuation algorithm starts from a known solution and uses a predictor-corrector scheme to find subsequent solutions at different load levels. While the corrector is nothing more than a slightly modified Newton-Raphson power flow, the predictor is quite unique from anything found in a conventional power flow and deserves detailed attention.

Once a base solution has been found ($\lambda = 0$), a prediction of the next solution can be made by taking an appropriately sized step in a direction tangent to the solution path. Thus, the first task in the predictor process is to calculate the tangent vector. This tangent calculation is derived by first taking the derivative of both sides of the power flow equations.

$$d[F(\underline{\delta}, \underline{V}, \lambda)] = F_{\underline{\delta}} d\underline{\delta} + F_{\underline{V}} d\underline{V} + F_{\lambda} d\lambda = \underline{0} \quad (11)$$

Factorizing

$$\begin{bmatrix} F_{\underline{\delta}} & F_{\underline{V}} & F_{\lambda} \end{bmatrix} \begin{bmatrix} d\underline{\delta} \\ d\underline{V} \\ d\lambda \end{bmatrix} = \underline{0} \quad (12)$$

On the left side of this equation is a matrix of partial derivatives multiplied by a vector of differentials. The former is the conventional load flow Jacobian augmented by one column (F_{λ}), while the latter is the tangent vector being sought. There is, however, an important barrier to overcome before a unique solution can be found for the tangent vector. The problem arises from the fact that one additional unknown was added when λ was inserted into the power flow equations, but the number of equations remained unchanged. Thus, one more equation is needed.

This problem can be solved by choosing a non-zero magnitude (say one) for one of the components of the tangent vector. In other words, if \underline{t} is used to denote the tangent vector;

$$\underline{t} = \begin{bmatrix} d\underline{\delta} \\ d\underline{V} \\ d\lambda \end{bmatrix}, \quad t_k = \pm 1 \quad (13)$$

This results in

$$\begin{bmatrix} F_{\underline{\delta}} & F_{\underline{V}} & F_{\lambda} \\ & & \underline{e}_k \end{bmatrix} \underline{t} = \begin{bmatrix} \underline{0} \\ \pm 1 \end{bmatrix} \quad (14)$$

Where \underline{e}_k is an appropriately dimensioned row vector with all elements equal to zero except the k^{th} , which equals one. If the index k is chosen correctly, letting $t_k = \pm 1$ imposes a non-zero norm on the tangent vector and guarantees that the augmented Jacobian will be non-singular at the critical point. Whether +1 or -1 is used depends on how the k^{th} state variable is changing as the solution path is being traced. If it is increasing, a +1 should be used and if it decreasing a -1 should be used. To know more about the state variables, refer to [2]. A method for choosing k and the sign of t_k will be presented later in the paper.

Once the tangent vector has been found by solving, the prediction can be made as follows:

$$\begin{bmatrix} \underline{\delta}^* \\ \underline{V}^* \\ \lambda^* \end{bmatrix} = \begin{bmatrix} \underline{\delta} \\ \underline{V} \\ \lambda \end{bmatrix} + \sigma \begin{bmatrix} d\underline{\delta} \\ d\underline{V} \\ d\lambda \end{bmatrix} \quad (15)$$

Where “*” denotes the predicted solution for a subsequent value of λ (loading) and σ is a scalar that designates the step size. The step size should be chosen so that the predicted solution is within the radius of convergence of the corrector.

D. THE REDUCED JACOBIAN TECHNIQUE

The technique implements a simple computation on the elements of the reduced Jacobian to find the suitable bus for capacitor placement as seen in the later section. The reduced Jacobian [6] is formulated from the Jacobian of the load flow. A brief description of the formulation of the reduced Jacobian is given before proceeding further.

Equation 3 gives the known matrix model of the load flow.

$$\begin{bmatrix} \Delta P \\ \Delta Q \end{bmatrix} = \begin{bmatrix} J_1 & J_2 \\ J_3 & J_4 \end{bmatrix} \begin{bmatrix} \Delta \Theta \\ \Delta V \end{bmatrix} \quad (16)$$

P and Q are the active and reactive power injections,

V and θ are the state variable vectors, namely voltage magnitude and bus angle, respectively,

ΔP is the difference in active power injection, ΔQ is the difference in reactive power injection,

$\Delta \Theta$ is the change in bus angle, ΔV is the change in bus voltage magnitude,

The reduced Jacobian used in this technique assumes that change in active load i.e. $\Delta P = 0$. Substituting this in (16), we get

$$J_1 \Delta \Theta + J_2 \Delta V = 0 \quad (17)$$

$$J_3 \Delta \Theta + J_4 \Delta V = \Delta Q \quad (18)$$

Putting $\Delta\theta$ from (17) in (18), we get

$$\Delta Q = (J_4 - J_3 J_1^{-1} J_2) \Delta V \quad (19)$$

$$\Delta Q = J_R \Delta V \quad (20)$$

$$\Delta V = J_R^{-1} \Delta Q \quad (21)$$

where J_R is reduced Jacobian.

The reduced Jacobian J_R gives a relationship describing ΔQ in terms of ΔV [1,6]. The inverse describes ΔV in terms of ΔQ . The elements in each column of the inverse matrix J_R^{-1} can be made to represent the change in voltage of every load bus for a given injection of reactive power into the bus corresponding to that column. The concept can be explained using a sample matrix like the one in (22) which shows J_R^{-1} as a (3 X 3) matrix.

A_{11}, A_{21}, A_{31} represent partial derivatives of voltages of load buses 1, 2 and 3 of the system with respect to reactive power at load bus i ,

ΔQ represents the vector of change in reactive power modeled by a fixed amount of reactive power injection, ΔV represents the vector of change in voltage.

This implies that for studying the change in voltage ΔV as a result of the reactive power injection into load buses separately or individually, the corresponding element of ΔQ , say ΔQ_i alone must be made 1 p.u. and the others 0. Upon implementing this, the corresponding column i in J_R^{-1} directly gives ΔV . Thus one needs to only study the elements of the particular column i of the reduced Jacobian to get the change in voltage as an effect of 1 p.u. reactive power injection at that bus i .

$$\left. \begin{aligned} A_{1i} &= \Delta V_1 \\ A_{2i} &= \Delta V_2 \\ A_{3i} &= \Delta V_3 \end{aligned} \right\} \quad (23)$$

The sum of the elements of that column i of J_R^{-1} further gives the total improvement of system voltage ΔV_{total_i} as an effect of the injection at the bus i . This is shown in (24).

$$A_{1i} + A_{2i} + A_{3i} = \Delta V_{total_i} \quad (24)$$

On comparison of the sums of all individual columns of J_R^{-1} the bus corresponding to the column i which yields maximum ΔV_{total_i} is determined as the bus required.

$$bus_i : \Delta V_{total_i} = \max \{ \Delta V_{total_1}, \Delta V_{total_2}, \Delta V_{total_3} \} \quad (25)$$

corresponding to the matrix given in (22).

bus_i is not the i^{th} bus in the system but the i^{th} load bus in the system as the buses involved in the analysis are only load buses.

It should be noted that the term $\Delta V_{overall}$ depicts the total improvement in system voltage where as the individual change in the bus voltage information come with the individual elements of J_R^{-1} .

3. CASE STUDY – IEEE 30 BUS SYSTEM

3.1 System model

We used the IEEE 30 bus system shown in Fig. A2 in the Appendix, for the case study. The load bus data and line data are given in Table A1 and A2 respectively in the Appendix.

3.2 Simulation results and discussion

3.2.1 The Modified Continuation Load Flow

The continuation load flow was carried out using the IEEE 30 bus system. The algorithm was based on the equations formulated in section 2. Bus 26 was selected as the industrial load whose induction motors were increased to depict increment in loading. Based on [7] the aggregate motor model and parameters were obtained from individual motors whose parameters are shown in Table A3 as found in [8,9].

The number of induction motors to be aggregated was calculated from the scheduled active power at the predicted operating point at each step of the continuation load flow. Based on the aggregate motor parameters obtained, the IM load was then modeled using Artificial Neuro Fuzzy inference system as described in section 2 using the algorithm in Fig A1. The Neuro fuzzy model of the induction motor was then used in the predictor-corrector stages of the solution. This process was conducted until all the operating points were calculated. The results with different motor ratings is shown in figures 1 and 2. Figure 1 shows the PV curves for the industrial load, while figure 2 shows the QV curves for the same load bus.

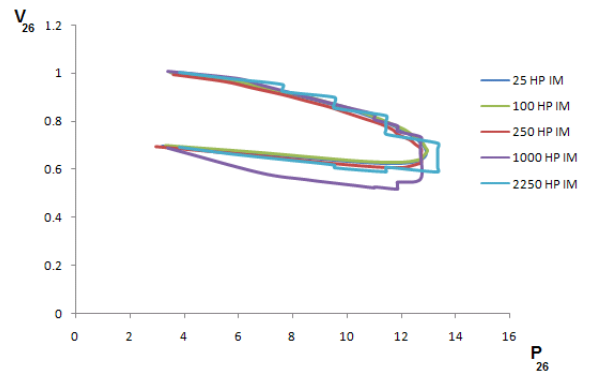


Figure 1. PV curve for bus 26 with different induction motor ratings

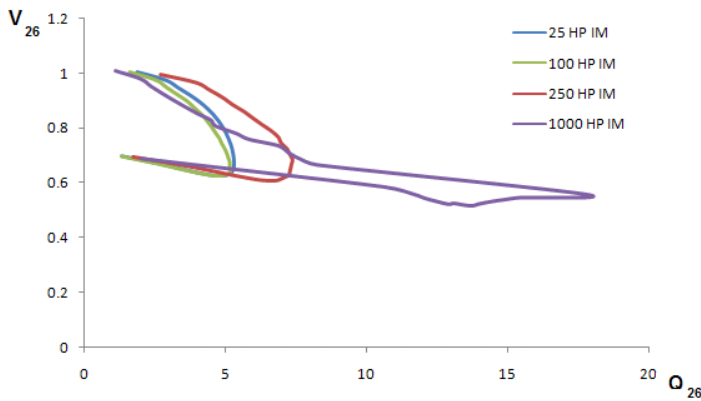


Figure 2. QV curve for bus 26 with different induction motor ratings

3.2.2 Optimal Capacitor Bank Placement

Based on the reduced Jacobian technique the optimal bus to place a capacitor bank was determined. In order to achieve these, the following extension was adopted [1]:

- Obtain subsequent operating points with continuation power flow.
- Obtain the matrix J_R and its inverse from the Jacobian of this operating point.
- Perform the same computations as discussed in the previous section and obtain the bus location.
- Repeat the previous steps for points consequent enough to cover a continuous range of operating points upto the maximum loading point.

Using the above the following results were achieved as shown in figure 3.

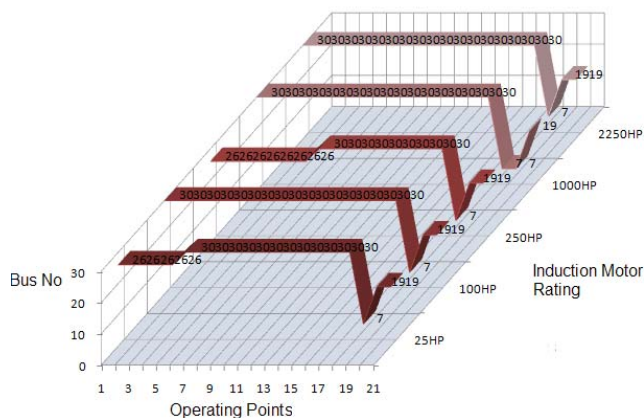


Figure 3. Optimal capacitor bank placement over operating points range

4. CONCLUSIONS

The modified continuation load flow with an neuro fuzzy induction motor clear shows that though the PV curves have almost similar maximum operating points, the QV curves are significantly different for different motors.

The actual situation with an induction motor load indicated that larger motors operate at low slips in normal rated operations, and hence consume less reactive power. But as the operating points move towards the critical loading and lower voltages, large motors draw more reactive power and hence pose as a greater threat to voltage stability of a system compared to their smaller counter parts. Thus depending on what kind of motor ratings are connected to a particular industrial load, the voltage stability risk is different. The smoothness of the PV curve is distorted when large motors are added to depict increment in loading.

The smoothness of the PV curve is distorted when large motors are added to depict increment in loading. This is because while in the normal continuation load flow, load increment is performed in small steps, in this modified algorithm, the increment is depicted by the individual horse power ratings of the induction motors being aggregated. Smaller increments lead to a smooth curve, while the large motor ratings are bound to distort that smoothness.

The reduced Jacobian technique successfully allocated the optimal bus for capacitor placement at each of the operating points plotted by the continuation power flow. This serves as a picture to let know the bus location fit enough for optimum voltage recovery for a particular operating point given a particular industrial load.

REFERENCES

- [1] Sivaramakrishnan R, Amit J, M. Ramamoorthy, Ashok V, A Methodology for Selective Localization of Capacitor Banks for Power Systems, Third International Conference on Power Systems, Kharagpur, 2009 , p 318
- [2] Venkataramana Ajjarapu, Iowa State University, "Computational techniques for voltage stability assessment and control", Springer, 2006.
- [3] Muriithi C. M., Ngoo L. M., Nyakoe G. N, "Load Flow Analysis With A Neuro-Fuzzy Model Of An Induction Motor Load", IEEE AFRICON 2009
- [4] Sadaat Hadi, "Power System Analysis", McGraw-Hill, -P 691, 2002.
- [5] Ricardo M. H, Nelson M, Julio C.R.F, Antonio C. B. M, Herminio J.C.P.P, Sandoval C. Jr, Impact of Induction motor Loads into Voltage Stability Margins of Large Systems -Rio Area Analysis, VIII SEPOPE, 2002
- [6] P Kundur, Power System Stability and Control, McGraw-Hill, pp 959-1022, 1994
- [7] P. Pillay, S.M.A. Sabur, M.M. Haq, A Model For Induction Motor Aggregation For Power System Studies, Electrical Power System Research, pages 225-228, 1997
- [8] Franklin, D. C, Morelato A., Improving Dynamic Aggregation of Induction Motor Models, IEEE Transactions on Power Systems, Vol. 9, No. 4, November 1994
- [9] Aree, P., Load flow solution with induction motor, Songklanakarin J. Sci. Technol., Vol.28 No.1, page 157-168., Jan. - Feb. 2006

APPENDIX

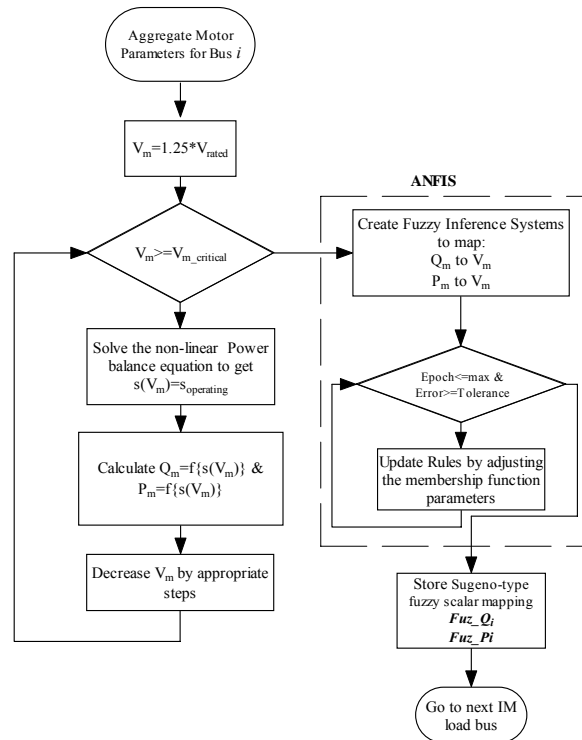


Figure A1: Algorithm for creating the neuro-fuzzy model of the induction motor

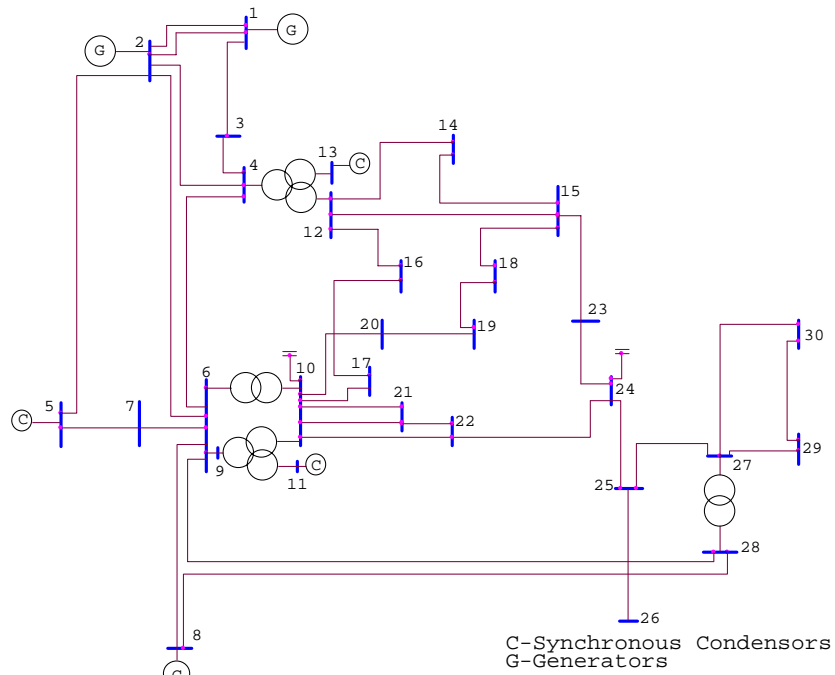


Figure A2

: IEEE 30-bus system

Table A1: IEEE 30 Bus system Load Bus Data

Bus No	Load	
	MW	MVAr
2	21.7	12.7
3	2.4	1.2
4	7.6	1.6
5	94.2	19
7	22.8	10.9
8	30	30
10	5.8	2
12	11.2	7.5
14	6.2	1.6
15	8.2	2.5
16	3.5	1.8
17	9	5.8
18	3.2	0.9
19	9.5	3.4
20	2.2	0.7
21	17.5	11.2
23	3.2	1.6
24	8.7	6.7
26	3.5	2.3
29	2.4	0.9
30	10.6	1.9

Table A2: IEEE 30 Bus system Line Data

Bus No	Bus No	R	X	B/2	Transformer tap setting
		pu	pu	pu	
1	3	0.0452	0.1852	0.0204	1
2	4	0.057	0.1737	0.0184	1
3	4	0.0132	0.0379	0.0042	1
2	5	0.0472	0.1983	0.0209	1
2	6	0.0581	0.1763	0.0187	1
4	6	0.0119	0.0414	0.0045	1
5	7	0.046	0.116	0.0102	1
6	7	0.0267	0.082	0.0085	1
6	8	0.012	0.042	0.0045	1
6	9	0	0.208	0	0.978
6	10	0	0.556	0	0.969

Bus No	Bus No	R	X	B/2	Transformer tap setting
9	11	0	0.208	0	1
9	10	0	0.11	0	1
4	12	0	0.256	0	0.932
12	13	0	0.14	0	1
12	14	0.1231	0.2559	0	1
12	15	0.0662	0.1304	0	1
12	16	0.0945	0.1987	0	1
15	18	0.1073	0.2185	0	1
18	19	0.0639	0.1292	0	1
19	20	0.034	0.068	0	1
10	20	0.0936	0.209	0	1
10	17	0.0324	0.0845	0	1
10	21	0.0348	0.0749	0	1
10	22	0.0727	0.1499	0	1
21	22	0.0116	0.0236	0	1
15	23	0.1	0.202	0	1
22	24	0.115	0.179	0	1
23	24	0.132	0.27	0	1
24	25	0.1885	0.3292	0	1
25	26	0.2544	0.38	0	1
25	27	0.1093	0.2087	0	1
28	27	0	0.396	0	0.968
27	29	0.2198	0.4153	0	1
27	30	0.3202	0.6027	0	1
29	30	0.2399	0.4533	0	1
8	28	0.0636	0.2	0.0214	1
6	28	0.0169	0.0599	0.065	1
14	15	0.221	0.1997	0	1
16	17	0.0824	0.1923	0	1

Table A3. Induction motor parameters based on individual Horse Powers (HP) (f=60Hz)

HP	Rs	Rr	Xs	Xr	Xm
25	0.0219	0.0472	0.0498	0.0498	1.9504
100	0.0109	0.0472	0.0532	0.0532	2.5121
250	0.0241	0.0141	0.0864	0.864	3.0263
1000	0.0158	0.0104	0.0851	0.0851	7.6343
2250	0.0092	0.0071	0.0718	0.0718	4.1388